Int. J. Solids Structures Vol. 26, No. 8, pp. 833–849, 1990
Printed in Great Britain.

0020–7683/90 $3.00 + .00

ASYMMETRIC BOUNDARY-VALUE PROBLEMS FOR A TRANSVERSELY ISOTROPIC ELASTIC MEDIUM

Y. WANG and R. K. N. D. RAJAPAKSE
Department of Civil Engineering, University of Manitoba, Winnipeg, Canada R3T 2N2

(*Received* 7 *April* 1989; *in revised form* 28 *September* 1989)

Abstract—This paper considers general boundary-value problems (displacement, traction, mixed) related to a transversely isotropic elastic half-space. The geometry of the problems considered is axisymmetric but the load is asymmetric. A cylindrical coordinate system is employed in the analysis and Fourier expansion and Hankel integral transforms are applied with respect to circumferential and radial coordinates, respectively. The boundary-value problems are formulated in terms of a system of non-singular integral equations for each Fourier harmonic. The kernels of the integral equations are displacement and traction Green's functions corresponding to buried ring loads with appropriate circumferential dependence. In general a total of 18 Green's functions are required for each Fourier harmonic. Explicit solutions for Green's functions corresponding to an arbitrary Fourier harmonic are presented in terms of infinite integrals of Lipschitz–Hankel type. The versatility of the solution scheme is illustrated by solving a traction boundary-value problem corresponding to a pressurized hemispherical cavity, displacement boundary-value problems related to an embedded rigid cylindrical body and a non-linear mixed boundary-value problem corresponding to an embedded rigid hemisphere with an elastic–perfectly plastic interface.

INTRODUCTION

Theoretical idealizations adopted to analyze a variety of problems encountered in geomechanics, fibre-reinforced composites and in micro-mechanics defects in solids often reduce to the solution of a boundary-value problem involving a transversely isotropic semi-infinite or an infinite elastic medium. The geometries relevant to many practical applications are axisymmetric but involve loading and boundary conditions which do not preserve axial symmetry. Muki (1960) presented a complete general solution for asymmetric deformations of an isotropic elastic solid by employing Hankel integral transforms and Fourier expansion with respect to radial and circumferential coordinates, respectively. Three-dimensional linear elasticity problems in transversely isotropic elastic materials have been studied, among others, by Elliott (1948), Hu (1954), Eubanks and Sternberg (1954), Stroh (1962), Lekhnitskii (1963), Chen (1966), Green and Zerna (1968), and Pan and Chou (1976, 1979). These studies were restricted to the derivation of general solutions for transversely isotropic media in terms of potential functions and the application of the general solutions to derive fundamental solutions corresponding to point forces acting in infinite and semi-infinite transversely isotropic media.

The majority of problems encountered in engineering applications of transversely isotropic materials involve complicated boundary and loading conditions. Some common examples are analysis of axisymmetric rigid inclusions embedded in transversely isotropic media, load-transfer from an elastic bar into a transversely isotropic medium, axisymmetric cavities subjected to arbitrary loading, and analytical model used to simulate *in situ* and non-destructive testing methods. Asymmetric boundary-value problems related to a transversely isotropic elastic half-space can be categorized as displacement, traction and mixed (displacement and traction) boundary-value problems. A review of existing literature indicates that a complete treatment of general boundary-value problems related to a three-dimensional transversely isotropic medium has not appeared in the literature. A class of traction boundary-value problems related to a two-dimensional orthotropic plane material was considered by Vable and Sikarskie (1988).

The main objective of this article is to develop a solution scheme for the analysis of displacement, traction and mixed boundary-value problems related to a transversely isotropic elastic half-space. To facilitate the analysis it is assumed that the geometry of the problem is axisymmetric. A cylindrical polar coordinate system together with Fourier

expansion in the circumferential direction is used in the analysis. Since any arbitrary displacement and traction boundary condition over an axisymmetric surface can be expressed in terms of a Fourier expansion the analysis needs to be presented only for a single arbitrary Fourier harmonic. The boundary-value problems are formulated in terms of a system of non-singular integral equations by generalizing the indirect boundary integral equation approach proposed by Ohsaki (1973) to study the response of a rigid body embedded in an isotropic elastic medium. The kernel functions of integral equations are displacement and traction Green's functions corresponding to a set of circular ring loads with appropriate circumferential dependence and acting in the interior of a transversely isotropic elastic half-space. Due to the complexity of the Green's functions the associated integral equations are solved numerically. It is noted that a total of 18 displacement and traction Green's functions are required for each Fourier harmonic. These Green's functions are derived explicitly by using Hankel integral transforms and expressed in terms of Lipschitz–Hankel integrals involving the product of Bessel functions of the first kind.

The accuracy, convergence and stability of the solution scheme are verified through a numerical study. The versatility of the solution scheme is demonstrated by analyzing a traction boundary-value problem related to a pressurized hemispherical cavity in a transversely isotropic elastic half space, displacement boundary-value problems related to a partially embedded rigid body and a non-linear mixed boundary-value problem related to an embedded rigid hemisphere with an elastic–perfectly plastic interface.

GOVERNING EQUATIONS AND GENERAL SOLUTION

Consider a transversely isotropic elastic half-space, with a Cartesian coordinate system (x, y, z) and a cylindrical polar coordinate system (r, θ, z) chosen such that the z-axis is normal to the stress-free surface and parallel to the material axis of symmetry. The mechanical response of a transversely isotropic elastic medium is governed by five elastic constants c_{11}, c_{12}, c_{13}, c_{33} and c_{44} which relate stresses and strains referred to a rectangular Cartesian coordinate system in the following manner (Lekhnitskii, 1963):

$$\sigma_{xx} = c_{11}\varepsilon_{xx} + c_{12}\varepsilon_{yy} + c_{13}\varepsilon_{zz} \tag{1a}$$

$$\sigma_{yy} = c_{12}\varepsilon_{xx} + c_{11}\varepsilon_{yy} + c_{13}\varepsilon_{zz} \tag{1b}$$

$$\sigma_{zz} = c_{13}\varepsilon_{xx} + c_{13}\varepsilon_{yy} + c_{33}\varepsilon_{zz} \tag{1c}$$

$$\sigma_{xy} = (c_{11} - c_{12})\varepsilon_{xy} \tag{1d}$$

$$\sigma_{yz} = 2c_{44}\varepsilon_{yz} \tag{1e}$$

$$\sigma_{xz} = 2c_{44}\varepsilon_{xz}. \tag{1f}$$

Alternatively, the stresses and strains referred to a cylindrical polar coordinate system are related in the following manner:

$$\sigma_{rr} = c_{11}\varepsilon_{rr} + c_{12}\varepsilon_{\theta\theta} + c_{13}\varepsilon_{zz} \tag{2a}$$

$$\sigma_{\theta\theta} = c_{12}\varepsilon_{rr} + c_{11}\varepsilon_{\theta\theta} + c_{13}\varepsilon_{zz} \tag{2b}$$

$$\sigma_{zz} = c_{13}\varepsilon_{rr} + c_{13}\varepsilon_{\theta\theta} + c_{33}\varepsilon_{zz} \tag{2c}$$

$$\sigma_{r\theta} = (c_{11} - c_{12})\varepsilon_{r\theta} \tag{2d}$$

$$\sigma_{\theta z} = 2c_{44}\varepsilon_{\theta z} \tag{2e}$$

$$\sigma_{rz} = 2c_{44}\varepsilon_{rz}. \tag{2f}$$

It can be shown that (Green and Zerna, 1968), in the absence of body forces, the displacement and stress fields in a transversely isotropic linear elastic material, subjected to a state of asymmetric deformations about the axis of elastic symmetry, can be expressed in terms of three potential functions $\phi_i(r, \theta, z)$, $i = 1, 2, 3$ which are solutions of

$$\left[\Delta^2+\frac{\partial^2}{\partial z_i^2}\right]\phi_i(r,\theta,z)=0, \quad i=1,2,3. \tag{3}$$

where

$$\Delta^2=\frac{\partial^2}{\partial r^2}+\frac{1}{r}\frac{\partial}{\partial r}+\frac{1}{r^2}\frac{\partial^2}{\partial\theta^2} \tag{4a}$$

and

$$z_i=z/\sqrt{v_i}, \quad i=1,2,3. \tag{4b}$$

In eqns (4b), v_1 and v_2 are the roots of the equation

$$c_{11}c_{44}v^2+[c_{13}(2c_{44}+c_{13})-c_{11}c_{33}]v+c_{33}c_{44}=0 \tag{5}$$

and v_3 is given by

$$v_3=\frac{2c_{44}}{(c_{11}-c_{12})}. \tag{6}$$

The roots v_1 and v_2 may be real or complex conjugates depending on the elastic constants c_{11}, c_{12}, c_{13}, c_{33} and c_{44}. Since the displacements and stresses must be real, the potential functions ϕ_1 and ϕ_2 are complex conjugate when v_1 and v_2 are complex and in addition it is necessary to specify that $\sqrt{v_1}$ and $\sqrt{v_2}$ always have positive real parts.

The displacement and stress components referred to a cylindrical polar coordinate system are given by:

$$u_r=\frac{\partial}{\partial r}(\phi_1+\phi_2)+\frac{1}{r}\frac{\partial\phi_3}{\partial\theta} \tag{7a}$$

$$u_\theta=\frac{1}{r}\frac{\partial}{\partial\theta}(\phi_1+\phi_2)-\frac{\partial\phi_3}{\partial r} \tag{7b}$$

$$u_z=\frac{\partial}{\partial z}(k_1\phi_1+k_2\phi_2) \tag{7c}$$

and

$$\frac{\sigma_{rr}}{c_{44}}=-\left[\lambda_1\frac{\partial^2\phi_1}{\partial z_1^2}+\lambda_2\frac{\partial^2\phi_2}{\partial z_2^2}\right]-\frac{2}{v_3}\left[\left(\frac{1}{r}\frac{\partial}{\partial r}+\frac{1}{r^2}\frac{\partial^2}{\partial\theta^2}\right)(\phi_1+\phi_2)-\frac{\partial}{\partial r}\left(\frac{1}{r}\frac{\partial\phi_3}{\partial\theta}\right)\right] \tag{8a}$$

$$\frac{\sigma_{\theta\theta}}{c_{44}}=-\left[\lambda_1\frac{\partial^2\phi_1}{\partial z_1^2}+\lambda_2\frac{\partial^2\phi_2}{\partial z_2^2}\right]-\frac{2}{v_3}\left[\frac{\partial^2}{\partial r^2}(\phi_1+\phi_2)+\frac{\partial}{\partial r}\left(\frac{1}{r}\frac{\partial\phi_3}{\partial\theta}\right)\right] \tag{8b}$$

$$\frac{\sigma_{zz}}{c_{44}}=\lambda_1 v_1\frac{\partial^2\phi_1}{\partial z_1^2}+\lambda_2 v_2\frac{\partial^2\phi_2}{\partial z_2^2} \tag{8c}$$

$$\frac{\sigma_{r\theta}}{c_{44}}=\frac{2}{v_3}\left(\frac{1}{r}\frac{\partial^2}{\partial r\,\partial\theta}-\frac{1}{r^2}\frac{\partial}{\partial\theta}\right)(\phi_1+\phi_2)+\frac{1}{v_3}\left(\frac{2}{r}\frac{\partial}{\partial r}+\frac{2}{r^2}\frac{\partial^2}{\partial\theta^2}+\frac{\partial^2}{\partial z_3^2}\right)\phi_3 \tag{8d}$$

$$\frac{\sigma_{\theta z}}{c_{44}}=\frac{1}{r}\frac{\partial}{\partial\theta}\left(\lambda_1\sqrt{v_1}\frac{\partial\phi_1}{\partial z_1}+\lambda_2\sqrt{v_2}\frac{\partial\phi_2}{\partial z_2}\right)-\frac{1}{\sqrt{v_3}}\frac{\partial^2\phi_3}{\partial r\,\partial z_3} \tag{8e}$$

$$\frac{\sigma_{rz}}{c_{44}}=\frac{\partial}{\partial r}\left(\lambda_1\sqrt{v_1}\frac{\partial\phi_1}{\partial z_1}+\lambda_2\sqrt{v_2}\frac{\partial\phi_2}{\partial z_2}\right)+\frac{1}{\sqrt{v_3}}\frac{1}{r}\frac{\partial^2\phi_3}{\partial\theta\,\partial z_3}, \tag{8f}$$

where

$$k_i = \frac{c_{11}v_i - c_{44}}{c_{13}+c_{44}}, \quad i = 1,2 \tag{9a}$$

$$\lambda_i = (1+k_i)/v_i, \quad i = 1,2. \tag{9b}$$

In order to determine a general solution for potential functions $\phi_i(r,\theta,z)$, $i = 1,2,3$ governed by eqn (3) the following representation is used:

$$\phi_i(r,\theta,z) = \sum_{m=0}^{\infty} [\phi_{im}(r,z)\cos m\theta + \bar{\phi}_{im}(r,z)\sin m\theta], \quad i = 1,2 \tag{10a}$$

$$\phi_3(r,\theta,z) = \sum_{m=0}^{\infty} [\phi_{3m}(r,z)\sin m\theta - \bar{\phi}_{3m}(r,z)\cos m\theta]. \tag{10b}$$

Substitution of eqn (10) in eqn (3) and subsequent application of Hankel integral transforms of order m (Sneddon, 1951) in the radial direction together with the orthogonality of trigonometric functions results in the following general solutions for Fourier harmonics of the three potential functions:

$$\phi_{im}(r,z) = \bar{\phi}_{im}(r,z) = \int_0^{\infty} [A_{im}(\xi)\,e^{\xi z_i} + B_{im}(\xi)\,e^{-\xi z_i}]\xi J_m(\xi r)\,d\xi, \quad i = 1,2,3. \tag{11}$$

In eqn (11), J_m denotes the Bessel function of the first kind of order m; ξ is the Hankel transform parameter; and $A_{im}(\xi)$ and $B_{im}(\xi)$ are arbitrary functions to be determined by using the given boundary conditions. Equations (7) and (8) together with eqns (10) and (11) represent the complete general solutions for arbitrary asymmetric deformations of a transversely isotropic elastic medium.

Note that in eqns (10), the first term produces deformations which are symmetric about $\theta = 0$ and the second term yields deformations that are antisymmetric with respect to $\theta = 0$. In the ensuing analysis we assume that $\bar{\phi}_{im} \equiv 0$ and consider solutions represented by only a single value of m in eqn (10) without loss of generality. It is noted that solutions corresponding to $\bar{\phi}_{im}$ can be obtained by making the replacements $\phi_{im} \to \bar{\phi}_{im}$, $\cos m\theta \to \sin m\theta$ and $\sin m\theta \to -\cos m\theta$.

GREEN'S FUNCTIONS

The derivation of displacement and traction Green's functions corresponding to circular ring loads acting in the interior of a transversely isotropic elastic half-space is considered in this section. These Green's functions appear as the kernel functions of the boundary integral equation formulation. In the derivation of Green's functions, ring loads acting in radial, circumferential and vertical directions are considered. The circumferential distribution of the radial and vertical ring loads is of the form $\cos m\theta$ and that of the circumferential load is $\sin m\theta$. The explicit solution for the Green's functions can be derived by defining a fictitious plane at the level of loading ($z = z'$) and treating the internally-loaded half-space as a two-domain problem (Chan *et al.*, 1974). The general solutions corresponding to each domain are given by eqns (7) and (8) together with eqn (11). In view of the prescribed circumferential distribution of the three ring loads only a single Fourier harmonic in eqn (10) need be considered. The Fourier harmonic of the displacements and stresses in each domain is denoted by $u_{\alpha m}^j$ ($\alpha = r,\theta,z$; $j = 1,2$) and $\sigma_{\alpha\beta m}^j$ ($\alpha,\beta = r,\theta,z$; $j = 1,2$), respectively. The superscript j denotes the domain number where domain "1" is bounded by $0 \leqslant z \leqslant z'$ and domain "2" by $z' \leqslant z < \infty$.

The boundary and continuity conditions corresponding to the three boundary-value problems involving the internally-loaded elastic half-space can be expressed as:

$$\sigma^1_{z\alpha m}(r,0) = 0, \quad \alpha = r,\theta,z \tag{12}$$

$$u^1_{\alpha m}(r,z') - u^2_{\alpha m}(r,z') = 0, \quad \alpha = r,\theta,z \tag{13}$$

$$\sigma^1_{z\alpha m}(r,z') - \sigma^2_{z\alpha m}(r,z') = F_\alpha, \quad \alpha = r,\theta,z. \tag{14}$$

For the radial loading case,

$$F_r = \delta(r-s) = \int_0^\infty \xi s J_m(\xi s) J_m(\xi r)\,\mathrm{d}\xi \tag{15a}$$

$$F_\theta = F_z = 0 \tag{15b}$$

where δ ( ) and s denote Dirac's delta function and the radius of the circular ring load, respectively.

For circumferential loading,

$$F_r = F_z = 0 \tag{16a}$$

$$F_\theta = \delta(r-s) = \int_0^\infty \xi s J_m(\xi s) J_m(\xi r)\,\mathrm{d}\xi. \tag{16b}$$

For vertical loading,

$$F_r = F_\theta = 0 \tag{17a}$$

$$F_z = \delta(r-s) = \int_0^\infty \xi s J_m(\xi s) J_m(\xi r)\,\mathrm{d}\xi. \tag{17b}$$

Substitution of general solutions for displacements and stresses in eqns (12)–(14) together with eqns (15)–(17) yields a set of linear simultaneous equations to determine arbitrary functions $A^j_{\alpha m}(\xi)$ and $B^j_{\alpha m}(\xi)$ $[\alpha = 1,2,3;\ j = 1,2]$ corresponding to the two domains. Note that $A^2_{\alpha m}(\xi) \equiv 0$ to ensure the regularity of displacements and stresses at infinity.

The explicit solutions for displacement Green's function $G^m_{\alpha\beta}(r,z;s,z')$ denoting the Fourier harmonic of the displacement in the α-direction ($\alpha = r,\theta,z$) at point (r,z) due to a ring load in the β-direction ($\beta = r,\theta,z$) with circumferential variation $\cos m\theta$ for $\beta = r,z$ and $\sin m\theta$ for $\beta = \theta$ through the point (s,z') can be expressed in the following form:

$$G^m_{rr}(r,z;s,z') = \bar{\mu}_1 \sum_{j=1}^{6} d_{3j}[I_j(m-1,m+1;0) - I_j(m+1,m+1;0) - I_j(m-1,m-1;0) + I_j(m+1,m-1;0)] + \bar{\mu}_2 \sum_{j=7}^{8} 4m^2 d_{3j} I^*_j(m,m;-2)/s \tag{18a}$$

$$G^m_{\theta r}(r,z;s,z') = -\bar{\mu}_1 \sum_{j=1}^{6} 2m d_{3j}[I^*_j(m,m+1;-1) - I^*_j(m,m-1;-1)] - \bar{\mu}_2 \sum_{j=7}^{8} 2m d_{3j}[\bar{I}_j(m+1,m;-1) - \bar{I}_j(m-1,m;-1)] \tag{18b}$$

$$G^m_{zr}(r,z;s,z') = 2\bar{\mu}_1 k_1 k_2 \sum_{j=1}^{6} d_{2j}[I_j(m,m+1;0) - I_j(m,m-1;0)] \tag{18c}$$

$$G^m_{r\theta}(r,z;s,z') = \bar{\mu}_1 \sum_{j=1}^{6} 2md_{3j}[\bar{I}_j(m-1,m;-1) - \bar{I}_j(m+1,m;-1)] + \bar{\mu}_2 \sum_{j=7}^{8} 2md_{3j}[I^*_j(m,m+1;-1) - I^*_j(m,m-1;-1)] \quad (19a)$$

$$G^m_{\theta\theta}(r,z;s,z') = -\bar{\mu}_1 \sum_{j=1}^{6} 4m^2 d_{3j} I^*_j(m,m;-2)/s - \bar{\mu}_2 \sum_{j=7}^{8} [I_j(m+1,m+1;0) - I_j(m-1,m+1;0) - I_j(m+1,m-1;0) + I_j(m-1,m-1;0)] \quad (19b)$$

$$G^m_{z\theta}(r,z;s,z') = 2\bar{\mu}_1 k_1 k_2 \sum_{j=1}^{6} 2md_{2j}\bar{I}_j(m,m;-1) \quad (19c)$$

$$G^m_{rz}(r,z;s,z') = 2\bar{\mu}_1 \sum_{j=1}^{6} d_{1j}[I_j(m-1,m;0) - I_j(m+1,m;0)] \quad (20a)$$

$$G^m_{\theta z}(r,z;s,z') = -2\bar{\mu}_1 \sum_{j=1}^{6} 2md_{1j} I^*_j(m,m;-1) \quad (20b)$$

$$G^m_{zz}(r,z;s,z') = 4\bar{\mu}_1 \sum_{j=1}^{6} \bar{v}_j d_{4j} I_j(m,m;0), \quad (20c)$$

where

$$\bar{\mu}_1 = \frac{s}{8c_{44}(k_1-k_2)}; \quad \bar{\mu}_2 = \frac{s\sqrt{v_3}}{8c_{44}} \quad (21)$$

$$d_{11} = d_{21} = -d_{12} = -d_{22} = \alpha; \quad d_{13} = d_{14} = -d_{23} = -d_{24} = \mu_2\mu_3 \quad (22a)$$

$$d_{15} = -d_{25}k_2/k_1 = -2\mu_2\sqrt{v_1}/\mu_4; \quad d_{16} = -d_{26}k_1/k_2 = -2\mu_2\mu_4\sqrt{v_2} \quad (22b)$$

$$d_{31} = k_2\sqrt{v_1}; \quad d_{32} = -k_1\sqrt{v_2}; \quad d_{33} = \mu_2\mu_3 k_2\sqrt{v_1} \quad (23a)$$

$$d_{34} = \mu_2\mu_3 k_1\sqrt{v_2}; \quad d_{35} = -2\mu_2 k_1\sqrt{v_1 v_2}/\mu_4 \quad (23b)$$

$$d_{36} = -2\mu_2\mu_4 k_2\sqrt{v_1 v_2}; \quad d_{37} = d_{38} = 1 \quad (23c)$$

$$d_{41} = -d_{42} = 1; \quad d_{43} = d_{44} = -\mu_2\mu_3; \quad d_{45} = 2\mu_2\sqrt{v_1}/\mu_4; \quad d_{46} = 2\mu_2\mu_4\sqrt{v_2} \quad (24)$$

$$\mu_1 = \frac{1}{k_1-k_2}; \quad \mu_2 = \frac{1}{\sqrt{v_2}-\sqrt{v_1}}; \quad \mu_3 = \sqrt{v_1}+\sqrt{v_2}; \quad \mu_4 = \frac{1+k_1}{1+k_2} \quad (25a)$$

$$\alpha = 1 \quad \text{if } z' \geqslant z$$
$$= -1 \quad \text{if } z' < z \quad (25b)$$

$$\bar{v}_j = \frac{k_1}{\sqrt{v_1}} \quad \text{for } j = 1,3,5$$
$$= \frac{k_2}{\sqrt{v_2}} \quad \text{for } j = 2,4,6 \quad (25c)$$

$$I_1(m,n;p) = \int_0^\infty J_m(\xi r)J_n(\xi s)\xi^p \, e^{-\xi|z_1-z_2|} \, d\xi \quad (26a)$$

$$I_2(m,n;p) = \int_0^\infty J_m(\xi r)J_n(\xi s)\xi^p \, e^{-\xi|z_2-z_2'|}\, d\xi \tag{26b}$$

$$I_3(m,n;p) = \int_0^\infty J_m(\xi r)J_n(\xi s)\xi^p \, e^{-\xi(z_1+z_1')}\, d\xi \tag{26c}$$

$$I_4(m,n;p) = \int_0^\infty J_m(\xi r)J_n(\xi s)\xi^p \, e^{-\xi(z_2+z_2')}\, d\xi \tag{26d}$$

$$I_5(m,n;p) = \int_0^\infty J_m(\xi r)J_n(\xi s)\xi^p \, e^{-\xi(z_1+z_2')}\, d\xi \tag{26e}$$

$$I_6(m,n;p) = \int_0^\infty J_m(\xi r)J_n(\xi s)\xi^p \, e^{-\xi(z_2+z_1')}\, d\xi \tag{26f}$$

$$I_7(m,n;p) = \int_0^\infty J_m(\xi r)J_n(\xi s)\xi^p \, e^{-\xi|z_3-z_3'|}\, d\xi \tag{26g}$$

$$I_8(m,n;p) = \int_0^\infty J_m(\xi r)J_n(\xi s)\xi^p \, e^{-\xi(z_3+z_3')}\, d\xi \tag{26h}$$

$$I_j^*(m,n;p) = I_j(m,n;p)/r, \quad j = 1,2,\ldots,8 \tag{27a}$$

$$\bar{I}_j(m,n;p) = I_j(m,n;p)/s, \quad j = 1,2,\ldots,8. \tag{27b}$$

For the case where deformations are also axisymmetric ($m = 0$), ring loads are considered only in the r- and z-direction and the displacement in the θ-direction is equal to zero. The relevant displacement Green's functions are given by eqns (18) and (20) with $m = 0$ and $G_{\theta r} = G_{\theta z} \equiv 0$.

The traction Green's function $H^m_{\alpha\beta}(r,z;s,z')$ denoting the Fourier harmonic of traction in the α-direction ($\alpha = r,\theta,z$) at a point (r,z) on a surface S with outward unit normal $\mathbf{n}$ due to a ring load in the β-direction ($\beta = r,\theta,z$) through the point (s,z') having circumferential variation $\cos m\theta$ for $\beta = r$ and z and $\sin m\theta$ for $\beta = \theta$ can be expressed as:

$$H^m_{\alpha\beta}(r,z;s,z') = \sigma^\beta_{\alpha jm}(r,z;s,z')n_j. \tag{28}$$

In eqn (28), summation is implied over index j ($j = r,\theta,z$) and $\sigma^\beta_{\alpha jm}(r,z;s,z')$ denotes the Fourier harmonic of the stress component $\sigma_{\alpha j}(\alpha, j = r,\theta,z)$ at point (r,z) due to a ring load in the β-direction ($\beta = r,\theta,z$) through the point (s,z') and n_j denotes the component of unit normal $\mathbf{n}$ in the j-direction. The explicit solutions for $\sigma^\beta_{\alpha jm}(r,z;s,z')$ are given below:

$$\begin{aligned}\sigma'_{rrm}(r,z;s,z') = \bar{\mu}_1 \sum_{j=1}^{6} d_{3j}\{&\bar{\lambda}_1(1+m)[I_j^*(m+1,m+1;0) - I_j^*(m+1,m-1;0)] \\ &+ \bar{\lambda}_1(1-m)[I_j^*(m-1,m-1;0) - I_j^*(m-1,m+1;0)] + 2\lambda_j[I_j(m,m-1;1) - I_j(m,m+1;1)]\} \\ &- \bar{\mu}_2 \sum_{j=7}^{8} 2m\bar{\lambda}_1[(1+m)I_j^*(m+1,m;-1) + (1-m)I_j^*(m-1,m;-1)]/s\end{aligned} \tag{29a}$$

$$\begin{aligned}\sigma'_{\theta\theta m}(r,z;s,z') = \bar{\mu}_1 \sum_{j=1}^{6} d_{3j}\{&\bar{\lambda}_1(1+m)[I_j^*(m+1,m-1;0) - I_j^*(m+1,m+1;0)] \\ &+ \bar{\lambda}_1(1-m)[I_j^*(m-1,m+1;0) - I_j^*(m-1,m-1;0)] \\ &+ 2(\bar{\lambda}_1 - \lambda_j)[I_j^*(m,m+1;1) - I_j^*(m,m-1;1)]\} \\ &+ \bar{\mu}_2 \sum_{j=7}^{8} 2m\bar{\lambda}_1[(1+m)I_j^*(m+1,m;-1) + (1-m)I_j^*(m-1,m;-1)]/s\end{aligned} \tag{29b}$$

$$\sigma^r_{zzm}(r,z;s,z') = 2\bar{\mu}_1 \sum_{j=1}^{6} (1+\omega_j) d_{3j}[I_j(m,m+1;1) - I_j(m,m-1;1)] \tag{29c}$$

$$\sigma^r_{r\theta m}(r,z;s,z') = \bar{\mu}_1 \sum_{j=1}^{6} d_{3j}\{\bar{\lambda}_1(1+m)[I^*_j(m+1,m+1;0) - I^*_j(m+1,m-1;0)]$$

$$+\bar{\lambda}_1(1-m)[I^*_j(m-1,m+1;0) - I^*_j(m-1,m-1;0)]\} + \bar{\mu}_2 \sum_{j=7}^{8} 2md_{3j}[-\bar{\lambda}_1 \bar{I}_j(m,m;0)$$

$$-\bar{\lambda}_1(1+m)I^*_j(m+1,m;-1) + \bar{\lambda}_1(1-m)I^*_j(m-1,m;-1)]/s \tag{29d}$$

$$\sigma^r_{\theta zm}(r,z;s,z') = 2\bar{\mu}_1 \sum_{j=1}^{6} md_{5j}\beta_j[I^*_j(m,m-1;0) - I^*_j(m,m+1;0)]$$

$$+\bar{\mu}_1 \sum_{j=7}^{8} 2md_{5j}[\bar{I}_j(m+1,m;0) - \bar{I}_j(m-1;m;0)]/\mu_1 \tag{29e}$$

$$\sigma^r_{zrm}(r,z;s,z') = \bar{\mu}_1 \sum_{j=1}^{6} d_{5j}\beta_j[I_j(m-1,m+1;1) - I_j(m+1,m+1;1) - I_j(m-1,m-1;1)$$

$$+I_j(m+1,m-1;1)] + \bar{\mu}_1 \sum_{j=7}^{8} 4m^2 d_{5j} I^*_j(m,m;-1)/s\mu_1 \tag{29f}$$

$$\sigma^\theta_{rrm}(r,z;s,z') = \bar{\mu}_1 \sum_{j=1}^{6} 2md_{3j}[\bar{\lambda}_1(1+m)I^*_j(m+1,m,-1)/s - \bar{\lambda}_1(1-m)I^*_j(m-1,m;-1)/s$$

$$-2\lambda_j \bar{I}_j(m,m;0)] + \bar{\mu}_2 \sum_{j=7}^{8} \bar{\lambda}_1\{(1+m)[I^*_j(m+1,m-1;0)$$

$$-I^*_j(m+1,m+1;0)] + (1-m)[I^*_j(m-1,m-1;0) - I^*_j(m-1,m+1;0)]\} \tag{30a}$$

$$\sigma^\theta_{\theta\theta m}(r,z;s,z') = \bar{\mu}_1 \sum_{j=1}^{6} 2md_{3j}[\bar{\lambda}_1(1-m)I^*_j(m-1,m;-1)/s - \bar{\lambda}_1(1+m)I^*_j(m+1,m;-1)/s$$

$$+2(\bar{\lambda}_1 - \lambda_j)\bar{I}_j(m,m;0)] + \bar{\mu}_2 \sum_{j=7}^{8} \lambda_1\{(1+m)[I^*_j(m+1,m+1;0) - I^*_j(m+1,m-1;0)]$$

$$+(1-m)[I^*_j(m-1,m+1;0) - I^*_j(m-1,m-1;0)]\} \tag{30b}$$

$$\sigma^\theta_{zzm}(r,z;s,z') = 2\bar{\mu}_1 \sum_{j=1}^{6} 2md_{3j}(1+\omega_j)\bar{I}_j(m,m;0) \tag{30c}$$

$$\sigma^\theta_{r\theta m}(r,z;s,z') = \bar{\mu}_1 \sum_{j=1}^{6} 2md_{3j}[\bar{\lambda}_1(1+m)I^*_j(m+1,m;-1)/s + \bar{\lambda}_1(1-m)I^*_j(m-1,m;-1)/s]$$

$$+\bar{\mu}_2 \sum_{j=7}^{8} d_{3j}\{\bar{\lambda}_1[I_j(m,m+1;1) - I_j(m,m-1;1)] + \bar{\lambda}_1(1+m)[I^*_j(m+1,m-1;0)$$

$$-I^*_j(m+1,m+1;0)] + \bar{\lambda}_1(1-m)[I^*_j(m-1,m+1;0) - I^*_j(m-1,m-1;0)]\} \tag{30d}$$

$$\sigma^\theta_{\theta zm}(r,z;s,z') = -\bar{\mu}_1 \sum_{j=1}^{6} 4m^2 d_{5j}\lambda_j I^*_j(m,m;-1)/s + \bar{\mu}_1 \sum_{j=7}^{8} d_{5j}[I_j(m+1,m+1;1)$$

$$+I_j(m-1,m-1;1) - I_j(m+1,m-1;1) - I_j(m-1,m+1;1)]/\mu_1 \tag{30e}$$

$$\sigma^\theta_{zrm}(r,z;s,z') = \bar{\mu}_1 \sum_{j=1}^{6} 2md_{5j}\lambda_j[\bar{I}_j(m-1,m;0) - \bar{I}_j(m+1,m;0)]$$

$$+\bar{\mu}_1 \sum_{j=7}^{8} 2md_{5j}[I^*_j(m,m+1;0) - I^*_j(m,m-1;0)]/\mu_1 \tag{30f}$$

$$\bar{\sigma}_{rrm}(r,z;s,z') = 2\bar{\mu}_1 \sum_{j=1}^{6} d_{1j}[\bar{\lambda}_1(1+m)I_j^*(m+1,m;0) - \bar{\lambda}_1(1-m)I_j^*(m-1,m;0) - 2\lambda_j I_j(m,m;1)] \quad (31a)$$

$$\bar{\sigma}_{\theta\theta m}(r,z;s,z') = 2\bar{\mu}_1 \sum_{j=1}^{6} d_{1j}[2(\bar{\lambda}_1-\lambda_j)I_j(m,m;1) - \bar{\lambda}_1(1+m)I_j^*(m+1,m;0) + \bar{\lambda}_1(1-m)I_j^*(m-1,m;0)] \quad (31b)$$

$$\bar{\sigma}_{zzm}(r,z;s,z') = 4\bar{\mu}_1 \sum_{j=1}^{6} d_{1j}(1+\omega_j)I_j(m,m;1) \quad (31c)$$

$$\bar{\sigma}_{r\theta m}(r,z;s,z') = 2\bar{\mu}_1 \sum_{j=1}^{6} d_{1j}[\bar{\lambda}_1(1+m)I_j^*(m+1,m;0) + \bar{\lambda}_1(1-m)I_j^*(m-1,m;0)] \quad (31d)$$

$$\bar{\sigma}_{\theta zm}(r,z;s,z') = -4\bar{\mu}_1 \sum_{j=1}^{6} m d_{4j}\beta_j I_j^*(m,m;0) \quad (31e)$$

$$\bar{\sigma}_{zrm}(r,z;s,z') = 2\bar{\mu}_1 \sum_{j=1}^{6} d_{4j}\beta_j[I_j(m-1,m;1) - I_j(m+1,m;1)], \quad (31f)$$

where

$$d_{51} = k_2\alpha\sqrt{\nu_1}; \quad d_{52} = -k_1\alpha\sqrt{\nu_2}; \quad d_{53} = -\mu_2\mu_3 k_2\sqrt{\nu_1}; \quad d_{54} = -\mu_2\mu_3 k_1\sqrt{\nu_2} \quad (32a)$$

$$d_{55} = 2\mu_2 k_1\sqrt{\nu_1\nu_2}/\mu_4; \quad d_{56} = 2\mu_2\mu_4 k_2\sqrt{\nu_1\nu_2}; \quad d_{57} = \alpha, \; d_{58} = -1 \quad (32b)$$

$$\bar{\lambda}_1 = \frac{c_{11}-c_{12}}{c_{44}}; \quad \bar{\lambda}_2 = \frac{1+k_1}{\nu_1}; \quad \bar{\lambda}_3 = \frac{1+k_2}{\nu_2}; \quad \bar{\lambda}_4 = \frac{1+k_1}{\sqrt{\nu_1}}; \quad \bar{\lambda}_5 = \frac{1+k_2}{\sqrt{\nu_2}} \quad (33)$$

$$\lambda_j = \bar{\lambda}_2; \quad \omega_j = k_1; \quad \beta_j = \bar{\lambda}_4 \quad \text{for } j = 1,3,5 \quad (34a)$$

$$\lambda_j = \bar{\lambda}_3; \quad \omega_j = k_2; \quad \beta_j = \bar{\lambda}_5 \quad \text{for } j = 2,4,6. \quad (34b)$$

Note that the displacement and traction Green's functions corresponding to transversely isotropic full space can be deduced directly from eqns (18)–(20) and (29)–(31) through an appropriate limit procedure.

FORMULATION OF BOUNDARY-VALUE PROBLEMS

Consider a transversely isotropic elastic half-space where a volume V bounded by an axisymmetric surface S is defined as shown in Fig. 1. A cylindrical polar coordinate system (r,θ,z) is defined at the free surface level such that the z-axis coincides with the axis of symmetry of V. If V is a rigid inclusion then displacements on S are prescribed and a displacement boundary-value problem can be defined for the semi-infinite transversely isotropic domain V_c exterior to V. If V is a cavity subjected to pressure then a traction boundary-value problem can be defined for the domain V_c. A more general situation exists when displacements are specified over a part of S denoted by S_1 (Fig. 1) and tractions are specified over the remainder of S denoted by S_2. In this case a mixed boundary-value

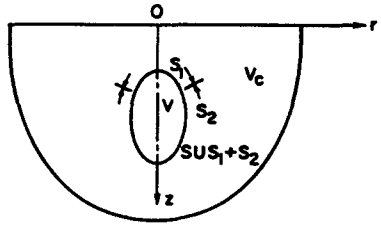

Fig. 1. Geometry of boundary-value problem.

problem can be defined for domain V_c. Examples of the mixed problem are situations where loss of contact exists over a portion of the contact surface of an inclusion in an elastic medium or the case of an inclusion where yielding occurs along the contact surface when tractions exceed prescribed limiting values.

In the ensuing analysis a detailed solution procedure for a traction boundary-value problem is presented. The solutions for displacement and mixed boundary-value problems can be developed by following similar procedures. Consider a situation where tractions are prescribed on a surface S as given below:

$$T_i(r,\theta,z) = \bar{T}_{im}(r,z) f_{im}(\theta), \quad (r,\theta,z) \in S. \tag{35}$$

In eqns (35), $i = r,\theta,z$ together with $f_{rm}(\theta) = f_{zm}(\theta) = \cos m\theta$ and $f_{\theta m}(\theta) = \sin m\theta$; $\bar{T}_{im}(r,z)$ denotes the prescribed value of traction on the generating curve of S.

An exact solution for domain V_c subjected to the above boundary condition on an arbitrary axisymmetric surface S is mathematically intractable. Alternatively, an indirect approach which exactly satisfies the governing equations of V_c and boundary conditions on S can be developed by considering a uniform (undisturbed) transversely isotropic elastic half-space V^* as shown in Fig. 2. An axisymmetric surface $\bar{S}$ which is identical to S in Fig. 1 is defined in V^*. Interior to $\bar{S}$, another axisymmetric surface S' is defined. A set of forces with intensity $B_i(r,z) f_{im}(\theta)$ is applied on S' such that tractions on $\bar{S}$ are given by eqn (35). Under these conditions the solution of domain $\bar{V}_c$ exterior to $\bar{S}$ is identical to that of V_c of the original problem. The force intensities $B_i(r,z)$ are governed by the following Fredholm integral equations of the first kind:

$$\int_{S'} H^m_{ij}(r,z;r',z') B_j(r',z') r' \, dS' = \bar{T}_{im}(r,z), \quad (r,z) \in S, \quad (r',z') \in S'. \tag{36}$$

In eqn (36), indices $i,j = r,\theta,z$ and summation is implied on j. In addition, $H^m_{ij}(r,z;r',z')$ denotes the traction Green's function defined by eqns (28)–(31) and S' refers to the generating curve of surface S'.

The unknown Fourier component of displacement on $\bar{S}$, denoted by $u_{im}(r,z)$, can be expressed as

$$\int_{S'} G^m_{ij}(r,z;r',z') B_j(r',z') r' \, dS' = u_{im}(r,z). \tag{37}$$

In view of the complexity of the Green's functions H^m_{ij}, eqns (36) are solved numerically. A discrete version of eqn (36) with respect to M and M' nodal points on $\bar{S}$ and S', respectively, can be expressed as:

$$[Q]\{B\} = \{R\}, \tag{38}$$

where

$$[Q] = [H] \tag{39}$$

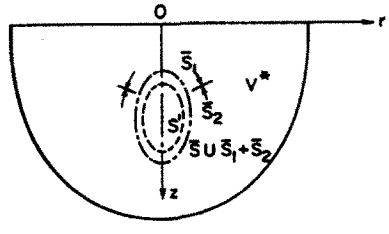

Fig. 2. Equivalent domain considered in the formulation.

$$[\bar{H}] = \begin{bmatrix} [\bar{H}_{rr}] & [\bar{H}_{r\theta}] & [\bar{H}_{rz}] \\ [\bar{H}_{\theta r}] & [\bar{H}_{\theta\theta}] & [\bar{H}_{\theta z}] \\ [\bar{H}_{zr}] & [\bar{H}_{z\theta}] & [\bar{H}_{zz}] \end{bmatrix}_{3M \times 3M'} \tag{40a}$$

$$[\bar{H}_{pq}] = [H^m_{pq}(r, z; r', z') r' \Delta S'], \quad p, q = r, \theta, z \tag{40b}$$

$$\{B\} = \langle\langle B_r(r', z')\rangle \quad \langle B_\theta(r', z')\rangle \quad \langle B_z(r', z')\rangle\rangle^{\mathrm{T}} \tag{41}$$

$$\{R\} = \langle\langle \bar{T}_{rm}(r', z')\rangle \quad \langle \bar{T}_{\theta m}(r', z')\rangle \quad \langle \bar{T}_{zm}(r', z')\rangle\rangle^{\mathrm{T}}. \tag{42}$$

In eqn (40), $[\bar{H}_{pq}]$ is a matrix whose elements are tractions in the p-direction of the nodes on $\bar{S}$ (unit normal as shown in Fig. 2) due to ring loads in the q-direction through node points on S'; $\Delta S'$ is the tributary length corresponding to a node point on S'; $\langle B_i(r', z')\rangle$ is a row vector whose elements are intensities of forces in the i-direction of the node point on S' and the superscript "T" denotes the transpose of a matrix.

A least-squares solution of eqn (38) yields

$$\{B\} = [[Q]^{\mathrm{T}}[Q]]^{-1}[Q]^{\mathrm{T}}\{R\}. \tag{43}$$

Once $\{B\}$ is determined from eqn (43), the Fourier harmonic of displacements on $\bar{S}$ (which are identical to displacements of S) can be computed by numerical integration of eqn (37).

In the case of a displacement boundary value problem, Fourier harmonic components of displacements on $S(\bar{S})$ are prescribed. The force intensities $B_i(r, z)$ are governed by the following Fredholm integral equation of the first kind:

$$\int_{S'} G^m_{ij}(r, z; r', z') B_j(r', z') r' \, \mathrm{d}S' = \bar{u}_{im}(r, z), \tag{44}$$

where $\bar{u}_{im}(r, z)$ denotes a prescribed displacement component on the generating curve of S.

A solution for $\{B\}$ is given by eqn (43) with

$$[Q] = [\bar{G}] \tag{45}$$

$$[\bar{G}] = \begin{bmatrix} [\bar{G}_{rr}] & [\bar{G}_{r\theta}] & [\bar{G}_{rz}] \\ [\bar{G}_{\theta r}] & [\bar{G}_{\theta\theta}] & [G_{\theta z}] \\ [\bar{G}_{zr}] & [\bar{G}_{z\theta}] & [\bar{G}_{zz}] \end{bmatrix} \tag{46a}$$

where

$$[\bar{G}_{pq}] = [G^m_{pq}(r, z; r', z') r' \Delta S']_{M \times M'} \quad p, q = r, \theta, z \tag{46b}$$

and

$$\{R\} = \langle\langle \bar{u}_{rm}(r', z')\rangle \quad \langle \bar{u}_{\theta m}(r', z')\rangle \quad \langle \bar{u}_{zm}(r', z')\rangle\rangle^{\mathrm{T}}. \tag{47}$$

The solution for traction components $T_{im}(r, z)$ is given by the following integral equation:

$$T_{im}(r, z) = \int_{S'} H^m_{ij}(r, z; r', z') B_j(r', z') r' \, \mathrm{d}S'. \tag{48}$$

In the case of mixed boundary-value problems tractions are prescribed over the part S_1 of S (Fig. 1) and displacements are prescribed over the remaining part $S_2[S \cup S_1 + S_2]$. Considering the system shown in Fig. 2, the force intensities $B_i(r', z')$ on S' are governed

by the following dual integral equation system:

$$\int_{S'} H_{ij}^{m}(r,z;r',z')B_j(r',z')r'\,dS' = \bar{T}_{im}(r,z), \quad (r,z)\in\bar{S}_1 \tag{49a}$$

$$\int_{S'} G_{ij}^{m}(r,z;r',z')B_j(r',z')r'\,dS' = \bar{u}_{im}(r,z), \quad (r,z)\in\bar{S}_2. \tag{49b}$$

A solution of eqn (49) to determine $\{B\}$ can be expressed in the form of eqn (43) by discretizing S_1 and S_2 by using M_1 and M_2 node points, respectively. The matrix $[Q]$ in eqn (43) corresponding to the present case can be expressed as:

$$[Q] = \begin{bmatrix}[\bar{H}]\\ [\bar{G}]\end{bmatrix} \tag{50}$$

where $[\bar{H}]$ and $[\bar{G}]$ are traction and displacement Green's function matrices defined by eqns (40) and (46), respectively. Note that the orders of $[\bar{H}]$ and $[\bar{G}]$ are $3M_1\times 3M'$ and $3M_2\times 3M'$, respectively. Once $\{B\}$ is known, the unknown displacement on S_1 and the unknown tractions on S_2 can be determined from eqns (44) and (48), respectively.

It should be mentioned here that the above boundary-value problems can also be analyzed by using the integral representation theorems (Rizzo, 1967; Eringen and Suhubi, 1975). The kernel functions of the resulting integral equations are again the displacement and traction Green's functions, given by eqns (18)–(20) and (28)–(31).

NUMERICAL RESULTS AND DISCUSSION

The numerical convergence, stability and accuracy of the solution scheme have been investigated with respect to two bench-mark problems for which solutions have been reported in the literature. The first problem is the completely axisymmetric traction boundary-value problem related to a spherical cavity of radius "a" in an isotropic infinite space which is subjected to a uniform radial pressure p_0. An exact analytical solution for this problem is available (Saada, 1974). The material isotropy is simulated by setting material constants $c_{11} = 3.0$, $c_{12} = 1.0$, $c_{33} = 3.0$, $c_{13} = 1.0$ and $c_{44} = 0.99997$. This corresponds to an isotropic material with shear modulus and Poisson's ratio equal to 1.0 and 0.25, respectively. Table 1 presents a comparison of displacement normal to the cavity wall denoted by Δ, for different location of inner surface S' (considered as a sphere of radius r^*) and different numbers of node points M and M'. The solutions obtained from the present scheme show good convergence and stable behaviour with increasing M and M' and are in very close agreement with the analytical solution. The second problem used in comparison is the asymmetric displacement boundary-value problem related to a rigid cylinder of radius "a"

Table 1. Variation of normal displacement of cavity wall for different location of S' and discretizations of S and S'

	$\mu\Delta/p_0a$	
(M', M)	$r^*/a = 0.75$	$r^*/a = 0.85$
(5, 10)	0.2120	0.1441
(6, 12)	0.2287	0.1718
(8, 12)	0.2438	0.2184
(8, 16)	0.2455	0.2241
(8, 18)	0.2459	0.2293
(10, 20)	0.2490	0.2319
(15, 30)	0.2499	0.2482
(20, 40)	0.2500	0.2497
Analytical	0.2500	

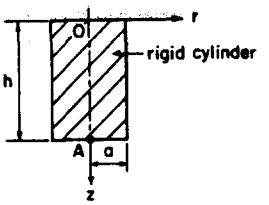

Fig. 3. Geometry of rigid cylinder embedded in a half-space.

and height "h" partially embedded in an isotropic elastic half-space (Fig. 3). The force–displacement relationship of the cylinder can be expressed in the form:

$$\begin{Bmatrix} F_0 \\ M_0/a \end{Bmatrix} = c_{44}a \begin{bmatrix} K_h & K_{hm} \\ K_{mh} & K_m \end{bmatrix} \begin{Bmatrix} \Delta_x \\ a\phi_y \end{Bmatrix}. \tag{51}$$

In eqn (51), K_h, K_m and K_{hm} ($= K_{mh}$) denote the non-dimensional horizontal, rocking and coupled stiffnesses of the rigid cylinder; Δ_x and ϕ_y denote the horizontal displacement (x-direction) of the bottom and rotation about the y-axis of the cylinder, respectively; F_0 and M_0 denote the resultant force in the x-direction and the bending moment about the y-axis with respect to the point A shown in Fig. 3, respectively.

Apsel and Luco (1987) presented solutions for rigid cylinders with various h/a ratios embedded in an isotropic elastic half-space (Poisson's ratio equal to 0.25) by numerically solving an integral equation scheme based on integral representation theorems (Eringen and Suhubi, 1975). Table 2 presents solutions for K_h, K_m and K_{hm} of a rigid cylinder with $h/a = 1$ for two location of surface S' [considered as a cylinder of radius r^* and height $(h-r^*)$] and for four different discretizations of $\bar{S}$ and S'. The convergence and the stability of the solution are clearly evident. Table 2 also presents a comparison with the solution presented by Apsel and Luco (1987). The above comparison confirms the accuracy, convergence and stability of numerical solutions obtained from the present analysis. In the ensuing sections, the versatility of the solution scheme is illustrated by solving traction, displacement and mixed boundary-value problems related to a transversely isotropic elastic half-space for which analytical solutions cannot be derived. The material properties (Chen, 1966; Payton, 1983) corresponding to transversely isotropic materials considered in this study are presented in Table 3, where $\bar{c}_{ij} = c_{ij}/c_{44}^{ice}$ and $c_{44}^{ice} = 0.317 \times 10^7\,\text{kN m}^{-2}$.

Table 2. Convergence of cylinder stiffnesses for various discretizations and locations of surface S'

	$r^* = 0.9$			$r^* = 0.85$		
(M, M')	K_h	$K_{mh} = K_{hm}$	K_m	K_h	$K_{mh} = K_{hm}$	K_m
(16, 8)	9.46	−2.87	13.48	9.49	−2.83	13.59
(24, 12)	9.51	−2.79	13.80	9.48	−2.81	13.75
(28, 14)	9.52	−2.78	13.88	9.51	−2.77	13.85
(32, 20)	9.52	−2.75	13.93	9.51	−2.77	13.92
Apsel and Luco (1987)	9.52	−2.75	13.94			

Table 3. Material constants of some transversely isotropic elastic media

	$\bar{c}_{11}$	$\bar{c}_{12}$	$\bar{c}_{13}$	$\bar{c}_{33}$	$\bar{c}_{44}$
Ice (275 K)	4.26	2.05	1.64	4.57	1.00
Cadmium	34.70	12.74	12.08	14.80	4.92
Magnesium	18.83	8.27	6.85	19.46	5.17
Clay I	0.147	0.053	0.037	0.103	0.031
Clay II	0.146	0.051	0.028	0.08	0.031
Isotropic*	3.0	1.0	1.0	3.0	0.99997

* Isotropic: $\nu = 0.25$, $\mu = 1.00$.

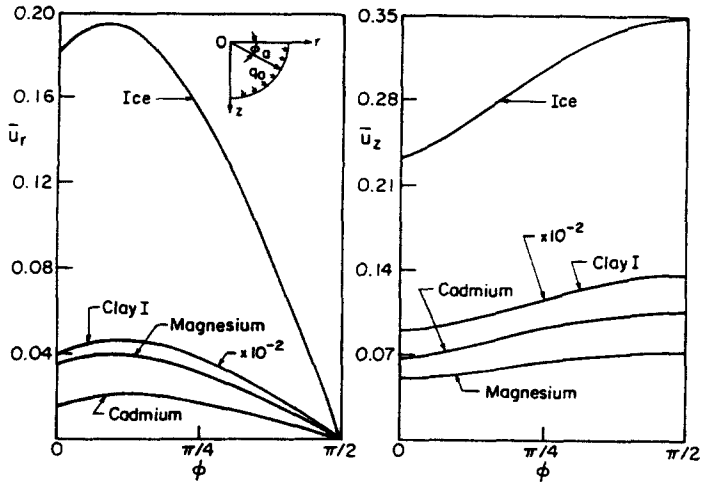

Fig. 4. Displacement profiles along hemispherical cavity surface.

Hemispherical cavity in transversely isotropic half-space

The traction boundary-value problem corresponding to a hemispherical cavity of radius "a" at the surface level of an elastic half-space is considered. The cavity is subjected to uniform normal pressure q_0. Figure 4 show the variation of the non-dimensional cavity wall. The material types considered are ice, clay, magnesium and cadmium. The solution presented in Fig. 4 corresponds to a surface S' of radius $0.75a$, and 20 and 40 node points on S' and S, respectively. A comparison of material constants presented in Table 3 indicates that among the materials considered in the present study ice and clay are softer than cadmium and magnesium. This observation is directly reflected in Fig. 4 where it is noted that displacements of a cavity in ice and clays are larger. The displacements of the clay cavity are the largest and plotted in Fig. 4 by using a scale factor of 10^{-2}. A comparison of displacement profiles corresponding to cadmium and magnesium shows interesting behaviour. The radial displacement of magnesium is larger than that of cadmium; however, the opposite is true for vertical displacements. It is noted from Table 3 and eqns (1) and (2) that cadmium has a greater stiffness in the $r\theta$ (xy) plane when compared to magnesium whereas the opposite is true for stiffness in the z-direction. This explains the behaviour of displacements noted in Fig. 4. The general variation of displacements along the cavity wall is roughly the same for all four materials although the actual magnitudes are considerably different. It is also evident that the degree of anisotropy of the material has a significant influence on the response. It should be mentioned here that the present scheme can analyze a cavity of any arbitrary axisymmetric geometry subjected to an arbitrary variation of pressure over the cavity surface. The Green's functions required in the analysis of a general case are given by eqns (18)–(20) and (28)–(31).

Rigid cylinder bonded to transversely isotropic half-space

The asymmetric displacement boundary-value problem related to a rigid cylinder bonded to a transversely isotropic elastic half-space is considered (Fig. 3). The problem under consideration has useful applications in geomechanics and in the analysis and design of mechanical components. The quantity of primary interest is the global stiffness of the cylinder–half-space system. Tables 3, 4 and 5 present non-dimensional axial (K_v), horizontal (K_h), rocking (K_m) and coupled ($K_{mh} = K_{hm}$) stiffnesses of a rigid cylinder bonded to ice, two types of clay and an isotropic medium. Note that $K_v = P_0/(c_{44}^{ice} a \Delta_z)$, where Δ_z is the displacement of the cylinder in the z-direction and P_0 is the axial force. The stiffnesses K_h, K_m, K_{hm} are defined by eqn (51) with $c_{44} = c_{44}^{ice}$. Solutions are presented for rigid cylinders with $h/a = 0.5$, 1.0, 2.0 and 4.0. As expected, all components' stiffnesses increase considerably with increasing values of the ratio h/a for all types of material. The stiffness values corresponding to the two clays are very close which indicates that the differences in $\bar{c}_{13}$ and

Table 4. Axial and horizontal stiffness of a rigid cylinder embedded in transversely isotropic elastic half-space

	K_v				K_h			
h/a	Ice	Clay I	Clay II	Isotropic	Ice	Clay I	Clay II	Isotropic
0.5	9.30	0.24	0.21	7.10	8.59	0.31	0.32	7.50
1.0	10.27	0.28	0.25	8.35	10.93	0.40	0.40	9.52
2.0	12.28	0.34	0.31	10.32	14.80	0.56	0.56	12.87
4.0	16.16	0.46	0.43	13.92	21.20	0.70	0.71	17.50

Table 5. Rocking and coupled stiffness of a rigid cylinder embedded in transversely isotropic half-space

	K_m				$-K_{mh} = -K_{hm}$			
h/a	Ice	Clay I	Clay II	Isotropic	Ice	Clay I	Clay II	Isotropic
0.5	9.37	0.25	0.24	7.65	0.93	0.04	0.03	0.73
1.0	16.40	0.51	0.49	13.93	3.31	0.12	0.12	2.75
2.0	42.08	1.45	1.43	36.37	10.59	0.39	0.39	9.06
4.0	160.28	5.53	5.56	131.04	33.65	1.37	1.37	25.76

$\bar{c}_{33}$ observed in Table 3 do not have a significant influence on the stiffness. A comparison of solutions corresponding to ice and the isotropic material indicates clearly the influence of the degree of anisotropy on the stiffness.

Rigid hemisphere with an elastic–perfectly plastic interface

The non-linear mixed boundary-value problem related to a rigid hemisphere of radius "a" embedded in a transversely isotropic elastic half-space with an elastic–perfectly plastic interface is considered. In the absence of relevant experimental data we have simulated only the axisymmetric twisting problem where yielding (slipping) occurs only in the θ-direction when contact traction reaches a limiting value. The limiting traction value in the θ-direction, denoted by $\tau_{\theta y}$, is set to 0.01 c_{44}. In reality the critical value of traction beyond which slipping occurs along the interface should be determined experimentally and depends on several factors such as the surface texture of the interface, the type of bonding, the deformability characteristics of the materials in contact, etc. The torque (T_0) and twist angle (ω_0) relationship is linear until the contract traction in the θ-direction at a point at the interface reaches the limiting value. A displacement boundary-value problem can be defined for domain V_c (Fig. 5) during the linear region. Let ω_y denote the twist angle (in radians) at the initiation of yielding. For any $\omega_0 > \omega_y$, a mixed boundary-value problem can be defined for V_c; the traction specified over the part where the critical value has been reached and the displacement specified over the remainder. Note that slipping will occur along the

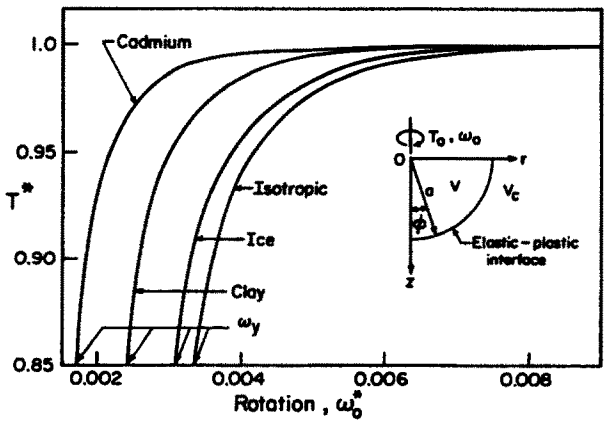

Fig. 5. Torque-twist relationship after initiation of interface yielding.

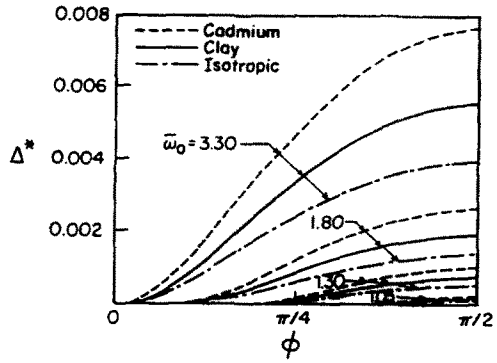

Fig. 6. Slip along the interface after initiation of interface yielding.

portion of the interface where the limiting traction has reached. It can be shown that the torque T_y corresponding to a completely yielded interface is equal to $0.005\pi^2 c_{44}a^3$ for $\tau_{\theta y} = 0.01\, c_{44}$. The response of the hemisphere for $\omega_0 > \omega_y$ can be studied by an incremental analysis. In the present study the surface S' was taken as a hemisphere of radius $0.8a$ and $M = 20$ and $M' = 10$. The incremental analysis was performed by using increments of rotation equal to $0.05\omega_y$ for $\omega_0 > \omega_y$.

Figure 5 shows the torque–twist relationship after the initiation of interface yielding for a rigid hemisphere embedded in an isotropic material, ice, clay and cadmium (Table 3). The point of intersection of the torque–twist curve with the horizontal axis corresponds to the twist angle ω_y at the initiation of interface yielding. The normalized torque $T^* = T_0/T_y$, where T_0 is the torque acting on the hemisphere and $\omega_0^* = \omega_0 c_{44}/\tau_{\theta y}$. The non-linear behaviour of the torque–twist relationship is evident from Fig. 5. The present analysis can be also used to compute the amount of slip between the rigid hemisphere and surrounding half-space at points along the interface which have reached the limiting traction. The non-dimensional slip at a point (r, z) on the interface is denoted by Δ^* and defined by $\Delta^*(r, z) = [r\omega_0 - v(r, z)]c_{44}/(a\tau_{\theta y})$, where $v(r, z)$ is the displacement in θ-direction of the half-space. Note that for $\omega_0 < \omega_y$, no slip takes place at the interface and $\Delta^* = 0$ for all points on the interface. Figure 6 shows the variation of Δ^* with the angle ϕ (Fig. 5) for normalized rotation $\bar{\omega}_0 = \omega_0/\omega_y$. Yielding is initiated at the free surface level ($\phi = \pi/2$) and gradually progresses downward as ω_0 is increased. Nearly one-half of the interface yields at $\bar{\omega}_0 = 1.30$ for all types of materials. Note that in the present problem, the analytical solution results in zero traction in the θ-direction as $\phi \to 0$. This implies, theoretically, the yielding of the bottom ($\phi = 0$) occurs when $\bar{\omega}_0 \to \infty$. This behaviour is reflected in both Figs 5 and 6. This example demonstrates the effectiveness of the present scheme in analysing a mixed boundary-value problem related to a rigid inclusion. The analysis can be modified without any fundamental difficulty to simulate an interface with Coulomb friction.

It can be concluded that an accurate boundary integral formulation has been presented to analyze a general (displacement, traction and mixed) boundary-value problem related to a transversely isotropic elastic medium. The Green's functions required in the analysis are presented explicitly. The numerical examples demonstrate the accuracy, flexibility and versatility of the solution scheme in analyzing a variety of problems. The traction–displacement relationship given by eqns (44)–(48) can be coupled to a finite element representation of the near field domain V to develop a hybrid scheme (Zienkiewicz *et al.*, 1977; Rajapakse and Shah, 1988) which can be used to model a variety of linear and non-linear problems related to transversely isotropic elastic media. The present methodology can be used to solve general boundary-value problems related to a multilayered transversely isotropic elastic medium without any fundamental difficulty. In the case of layered media, however, the Green's functions cannot be derived explicitly and have to be constructed by using accurate numerical techniques. Research in these directions is currently in progress for both static and dynamic problems.

Acknowledgement—The work presented here was supported by The Natural Sciences and Engineering Research Council of Canada, grant A-6507.

REFERENCES

Apsel, R. J. and Luco, J. E. (1987). Impedance functions for foundations embedded in a layered medium: an integral equation approach. *Earthquake Engng Struct. Dynam.* **15,** 213–221.

Chan, K. S., Karasudhi, P. and Lee, S. L. (1974). Force at a point in the interior of a layered elastic half space. *Int. J. Solids Structures* **10,** 1179–1199.

Chen, W. T. (1966). On some problems in transversely isotropic elastic materials. *J. Appl. Mech. ASME* **33,** 347–355.

Elliott, H. A. (1948). Three-dimensional stress distributions in hexagonal aeolotropic crystals. *Proc. Cambridge Philosophical Soc.* **44,** 522–533.

Eringen, A. C. and Suhubi, E. S. (1975). *Elastodynamics*, Vol. 2. Academic Press, New York.

Eubanks, R. A. and Sternberg, E. (1954). On the axisymmetric problem of elasticity theory for a medium with transverse isotropy. *J. Rational Mech. Analysis* **3,** 89–101.

Green, A. E. and Zerna, W. (1968). *Theoretical Elasticity*. Clarendon Press, Oxford, U.K.

Hu, H. C. (1954). On the equilibrium of a transversely isotropic elastic half-space. *Scientia Sinica* **3,** 463–479.

Lekhnitskii, S. G. (1963). *Theory of Anisotropic Elastic Bodies*. Holden-Day, San Francisco, CA.

Muki, R. (1960). Asymmetric problems of the theory of elasticity for a semi-infinite solid and a thick plate. In *Progress in Solid Mechanics* (Edited by I. N. Sneddon and R. Hill), Vol. 1, pp. 399–439. North Holland, Amsterdam.

Ohsaki, Y. (1973). On movement of a rigid body in a semi-infinite elastic medium. *Proc. Jap. Earthquake Engng Symp.*, Japan, 245–252.

Pan, Y. C. and Chou, T. W. (1976). Point force solution for an infinite transversely isotropic solid. *J. Appl. Mech., ASME* **43,** 1–5.

Pan, Y. C. and Chou, T. W. (1979). Green's function solutions for semi-infinite transversely isotropic materials. *Int. J. Engng Sci.* **17,** 545–551.

Payton, R. G. (1983). *Elastic Wave Propagation in Transversely Isotropic Media*. Martinus Nijhoff, The Netherlands.

Rajapakse, R. K. N. D. and Shah, A. H. (1988). Hybrid modelling of semi-infinite media. *Int. J. Solids Structures* **224,** 1205–1224.

Rizzo, R. J. (1967). An integral equation approach to boundary value problems in classical elastostatics. *Q. Appl. Math.* **25,** 83–95.

Saada, A. S. (1974). *Elasticity: Theory and Applications*. Pergamon Press, Oxford, U.K.

Sneddon, I. N. (1951). *Fourier Transforms*. McGraw-Hill, New York.

Stroh, A. N. (1962). Steady state problems in anisotropic elasticity. *J. Math. Physics* **41,** 77–103.

Vable, M. and Sikarskie, D. L. (1988). Stress analysis in plane orthotropic material by the boundary element method. *Int. J. Solids Structures* **24,** 1–11.

Zienkiewicz, O. C., Kelly, D. W. and Bettes, P. (1977). The coupling of the finite element and boundary solution procedures. *Int. J. Numer. Meth. Engng* **11,** 355–375.